Tolerance for local and global differences in the integration of shape information

J. Edwin Dickinson School of Psychology, University of Western Australia, Crawley, Perth, WA, Australia

Serena J. Cribb School of Psychology, University of Western Australia, Crawley, Perth, WA, Australia

Hugh Riddell School of Psychology, University of Western Australia, Crawley, Perth, WA, Australia

David R. Badcock School of Psychology, University of Western Australia, Crawley, Perth, WA, Australia

Shape is a critical cue to object identity. In psychophysical studies, radial frequency (RF) patterns, paths deformed from circular by a sinusoidal modulation of radius, have proved valuable stimuli for the demonstration of global integration of local shape information. Models of the mechanism of integration have focused on the periodicity in measures of curvature on the pattern, despite the fact that other properties covary. We show that patterns defined by rectified sinusoidal modulation also exhibit global integration and are indistinguishable from conventional RF patterns at their thresholds for detection, demonstrating some indifference to the modulating function. Further, irregular patterns incorporating four different frequencies of modulation are globally integrated, indicating that uniform periodicity is not critical. Irregular patterns can be handed in the sense that mirror images cannot be superimposed. We show that mirror images of the same irregular pattern could not be discriminated near their thresholds for detection. The same irregular pattern and a pattern with four cycles of a constant frequency of modulation completing 2π radians were, however, perfectly discriminated, demonstrating the existence of discrete representations of these patterns by which they are discriminated. It has previously been shown that RF patterns of different frequencies are perfectly discriminated but that patterns with the same frequency but different numbers of cycles of modulation were not. We conclude that such patterns are identified, near threshold, by the set of angles subtended at the center of the pattern by adjacent points of maximum convex curvature.

Introduction

The raw material from which the visual system is required to form an interpretation of the environment is an array of local luminous intensity measurements, converted within the retina to contrast in luminance and chromaticity. Color is not perceived under low levels of ambient luminance, yet the visual system is still able to make sense of the visual scene. It is evident, then, that spatial structure in the luminance contrast measurements is critical to that interpretation. At the level of the primary visual cortex, individual neurons are selective for orientation (Hubel & Wiesel, 1959, 1968), performing the role of oriented spatial filters for contrast in luminance or texture (a second-order property that might be described as a local contrast in luminance contrast (Badcock, 1988; Badcock & Derrington, 1989; Julesz, 1962). The response of adjacent and approximately collinearly arranged filters is enhanced by excitatory lateral connections in the event that both are simultaneously subject to appropriate stimuli (Field & Hayes, 2004; Field, Hayes, & Hess, 1993; Li & Gilbert, 2002). Under such circumstances, it is likely that the stimuli correspond to segments of an extended feature of the projected image of the environment. In this way, the salience of continuous paths is enhanced. The salience of closed paths is further enhanced (Kovacs & Julesz, 1993), suggesting that the visual field is parsed at the boundaries of objects, which are often characterized by a contrast in

Citation: Dickinson, J. E., Cribb, S. J., Riddell, H., & Badcock, D. R. (2015). Tolerance for local and global differences in the integration of shape information. *Journal of Vision, 15*(3):21, 1–24, http://www.journalofvision.org/content/15/3/21, doi:10.1167/15.3.21.

doi: 10.1167/15.3.21 Received May 18, 2014; published March 26, 2015 ISSN 1534-7362

luminance or texture across the boundary. Identification of objects, however, requires analysis of their shapes (Tan, Dickinson, & Badcock, 2013). A stimulus that has gained some prominence in the psychophysical literature pertaining to the study of shape is the radial frequency (RF) pattern (Almeida, Dickinson, Maybery, Badcock, & Badcock, 2010a, 2010b, 2013, 2014; Bell & Badcock, 2008; Bell, Badcock, Wilson, & Wilkinson, 2007; Dickinson, Almeida, Bell, & Badcock, 2010; Dickinson, Han, Bell, & Badcock, 2010; Dickinson, Harman, Tan, Almeida, & Badcock, 2012; Dickinson, McGinty, Webster, & Badcock, 2012; Dickinson, Mighall, Almeida, Bell, & Badcock, 2012; Loffler, 2008; Loffler, Wilson, & Wilkinson, 2003; Wilkinson, Wilson, & Habak, 1998). Such patterns are contours subtly deformed from circular by a sinusoidal modulation of radius. The number of cycles of modulation of a specific frequency of modulation is varied, and patterns with fewer than the requisite number of cycles of modulation to fill 2π radians are completed with a circular arc. As cycles of modulation of a particular frequency are added to RF patterns, the amplitude of modulation required for observers to be able to detect deformation of a pattern decreases at a rate faster than predicted by the increasing probability of detecting single cycles of modulation (probability summation). This has been interpreted as indicative of integration of shape information around the patterns (Loffler et al., 2003). RF patterns, then, provide stimuli that have demonstrably global shape representations and precisely specified shapes. By manipulating the amplitude and frequency of modulation and the number of cycles of that modulation, the relative importance of local properties such as the deviation of the local orientation of the contour from a circle and curvature of the pattern can be examined. Moreover, the widely used choice of the sinusoid as the modulating function is perhaps only a convenience, and the RF pattern, therefore, provides an ideal baseline for the exploration of other modulating functions in the investigation of shape processing in the visual system.

On the basis of perceptual studies, Attneave (1954) suggested that the points of maximum curvature on a boundary, the points of fastest rate of orientation change along the boundary, had the greatest information content, an argument supported by information theory (Feldman & Singh, 2005). Feldman and Singh (2005) also showed that the points on a closed path that are concave (indentations on the object) carry the highest information content. Hoffman and Richards (1984) and subsequently Biederman and Cooper (1991) have suggested that complex objects are decomposed at matched points that are concave. This reduces the image to shapes that are bounded by lines with occasional points of maximum convex curvature and one or no points of maximum concave curvature. RF patterns, having no points of concave curvature at their thresholds for detection, are therefore useful stimuli for the examination of the analysis of the components of shape by the visual system. Poirier and Wilson (2006) developed a model designed to account for psychophysical sensitivity to RF patterns in a biologically plausible manner. They measure curvature by determining the relationship between the local tangent to the contour and a line perpendicular to a radial line projecting from the center of the pattern. The rate of change of the angle between these two lines with polar angle is their measure of curvature around the pattern. This renders curvature invariant under a change in the size of the pattern. Their model, however, does not use negative curvature estimates calculated in this way. These negative estimates would indicate curves straighter than the circular arc or, for large amplitudes of modulation, concave to the outside of the pattern (in this formulation, a circle would have zero curvature). Their model, then, uses a size-invariant measure of curvature to identify points of maximum curvature.

Conventional measures of curvature on a path are specified in terms of the rate of change of orientation with path length rather than with polar angle measured with respect to a pattern center. It has been shown that such measures of local curvature, the rate of change of orientation with distance along a path in the Cartesian frame, can be made by combining the responses of simple cells of the primary visual cortex (V1) arranged at intervals along the curve (Wilson, 1985; Wilson & Richards, 1989) into spatial filters sensitive to particular configurations of V1 receptive fields (a straight line is defined as having zero curvature). Regardless of whether such local measures of curvature are made relative to a circular arc or relative to a straight line, if they measure a change in angle over an interval of path length, then curvature would be sensitive to the pattern radius. The threshold for detection of modulation in RF patterns is, however, a constant proportion of radius (Wilkinson et al., 1998), suggesting that the property of RF patterns that limits detection of RF patterns is not curvature as conventionally measured. One property of RF patterns that is size invariant is the maximum orientation deviation from circularity, and Dickinson, McGinty et al., (2012) have shown that, at threshold, RF patterns with different frequencies of modulation but the same number of cycles of modulation have the same magnitude of this quantity. In Experiment 1, we use rectified sinusoidal modulation of radius to create patterns that have the same maximum deviation from circularity but different curvature profiles to examine how curvature encoding enters the analysis of shape near the threshold for detection of that shape. We find that the shape information is integrated around rectified patterns despite the presence of curvature discontinuities and, in

the case of positively rectified patterns, concavities. Further, we find that thresholds are indeed constrained by orientation rather than curvature, placing important constraints on models of the processing of shapes at their thresholds for detection. In particular, this result challenges the assumption that the positions of points of maximum curvature on a boundary are necessarily determined by continuous measures of curvature.

Experiment 1 demonstrates that, like conventional RF patterns, patterns with rectified sinusoidal modulation of radius are globally processed. At threshold, patterns with the same number of cycles of modulation of radius completing the 2π radians were shown to have the same maximum orientation difference from circular. The orientation distributions for the three stimuli are different, but the maximum deviation from the orientation profile of a circle is the same for all three stimuli. That is to say that if the path was sampled for orientation deviation from circular on the curve, the orientation with respect to circular would differ locally around the pattern but the content of the orientation difference from circular would be identical. The maximum orientation difference from circular is the same for the patterns, but locally, the rate of change of orientation differs, whether measured as the rate of orientation with path length or polar angle. This implies that shape analysis at threshold relies on orientation difference from circular but is not critically dependent on the magnitude of curvature. By extension, this suggests that some analytical representation of shape is arrived at that is indifferent to the local properties from which it is derived. This conjecture is examined in Experiment 2 by testing whether the three pattern types could be discriminated at their thresholds for detection. Patterns with the same frequency of modulation of radius were used in a two-decision, two-interval, forced choice (2x2IFC) task (Watson & Robson, 1981). Evidence that the patterns were perfectly discriminated might suggest that shapes are labeled for the nature of the points of maximum convex curvature (i.e., smoothly curved or angles) or indeed were identified by any other local property, perhaps including the existence of points of infinite curvature (orientation discontinuities). However, the patterns are found to be not discriminable near their thresholds for detection. This suggests that the representations of shape arrived at, which are demonstrated to be global in Experiment 1, are indifferent to the local properties of the pattern. That is not to say that the local properties are unimportant to the analysis, as Experiment 1 also demonstrates the significance of local orientation difference from circular to the threshold for detection, but that the local information cannot be used in the discrimination task. This might indicate that, in the representation of shape, a perceptual decision has been made allowing for a more concise representation (Lennie, 1998).

The results of Experiment 2 demonstrate that patterns with the same frequency of modulation of radius but with sinusoidal or rectified sinusoidal modulation cannot be discriminated at their thresholds for detection. These patterns differ in their local radius (and amplitude of modulation), orientation, and curvature. One property that is common to the stimuli is the relative positions of the points of maximum convex curvature, and we propose that this is the predominant cue used to encode shape near threshold for detection. From this point, the model of Poirier and Wilson (2006) proceeds by analysis of the periodicity of measures of curvature that are convex with respect to the local circular arc. The shape is represented in the frequency spectrum of the curvature expressed with respect to polar angle. An implication of this proposed solution is that shape might be decomposed into RF components, perhaps via a bank of RF selective channels (although reconstruction of the pattern would also require the phase of the components to be encoded). This solution, however, is inconsistent with models of shape encoding for suprathreshold stimuli. Models of shape derived to account for the results of neurophysiological studies encode shape by the relative positions of salient curvature features on the boundary with respect to a pattern center (Connor, 2004; Pasupathy & Connor, 1999, 2001, 2002). These models require no periodicity in the positions of the points used in the analysis of shape. A boundary is traced as a trajectory through a two-dimensional space defined by the axes of curvature (measured conventionally as the rate of change of orientation with path length) and polar angle. Experiment 2 of this study demonstrates that, near detection threshold, the mechanisms encoding shape are indifferent to absolute measures of curvature and so, near detection threshold, the curvature versus polar angle space proposed by Connor et al. collapses to the positions of curvature features on the polar angle axis. Dickinson, Bell, and Badcock (2013), using a discrimination at threshold for detection paradigm in a two-decision, two-interval, forced choice (2x2IFC) task (Watson & Robson, 1981), showed that RF patterns with different modulation frequencies could be discriminated at their thresholds for the detection of modulation if they contained two or more cycles of modulation. Patterns with the same frequency but different numbers of cycles of modulation, however, could not. Evidence that discrimination is possible at threshold for detection, so called perfect discrimination, is indicative of the existence of information channels labeled for particular values of a property (Watson & Robson, 1981). These results were therefore interpreted as indicating that a critical cue to discrimination was the period of repetition of features on adjacent cycles of modulation and that this property is encoded in a bank of channels sensitive to the

subtended polar angle between adjacent curvature features. One can imagine that in the Poirier and Wilson (2006) model, the signal from repeated cycles of modulation would result in increasing amplitude in the RF spectrum at a particular frequency. Patterns with different frequencies of modulation would, obviously, have different spectra. This leads to an alternative interpretation of the Poirier and Wilson model, that the peaks on the spectrum, rather than representing a decomposition of the pattern into RF components, represent the polar angles subtended by adjacent points of maximum curvature. The shape might then be represented by the positions of the peaks in the spectrum. This solution is functionally equivalent to that proposed by Dickinson et al. (2013), that shape is encoded in the set of angles subtended at the center of the pattern by adjacent points of maximum curvature. This solution does not encode curvature but only the relative positions of points of maximum curvature. Experiment 3 tests this particular conjecture using irregular patterns. To recapitulate, Dickinson et al. (2013) showed that the critical difference that allowed RF patterns to be discriminated at their threshold for detection was a difference in the periodicity of repetition of points of maximum curvature, or corners, on the path (see also Bell, Dickinson, & Badcock, 2008), that is, differences in the angle subtended by adjacent points of maximum curvature at the center of the pattern. Patterns with different frequencies of modulation were perfectly discriminated provided that the patterns contained two or more cycles of modulation, and hence two points of maximum curvature, but patterns with different numbers of cycles of modulation with the same frequency were not. This result is indicative of the existence of information channels labeled for the angle subtended at the center of the pattern by adjacent corners on the path. A more natural complex shape, however, might have differing angles subtended by different pairs of adjacent corners. This raises the question of whether the integration around RF patterns occurs within such channels or across a bank of channels. Tests for integration of information around RF patterns have previously been restricted to patterns that have a constant period of modulation. Dickinson, McGinty et al., (2012), however, showed that thresholds for the detection of RF patterns with the same number of periods of modulation are inversely related to the frequency of modulation. Because the first derivative (gradient) of the sinusoid at its zero crossing is linearly related to the amplitude of modulation, patterns at their thresholds for modulation have the same first derivative at the mean radius of the pattern (or, for small amplitudes of modulation, the same angular deviation from circular at this point). By manipulating the amplitudes of modulation, we can create patterns with concatenated cycles of modulation with differing frequency and therefore patterns with different periods, or subtended angles between corners. Moreover, because of the compensating effects of amplitude and frequency of modulation, the individual cycles of differing period all have the same salience when presented in isolation. This then allows us to test for integration around patterns with an irregular distribution of corners. Experiment 3 tests for integration in these irregular patterns, and indeed, integration is observed.

Experiment 3, then, demonstrates that shape information is integrated around patterns with points of maximum curvature distributed irregularly with respect to polar angle. This does not, however, prove that the shapes are discriminable from other, different shapes, on the basis of this information. Experiment 4 examines the nature of the shape representation in light of the demonstration of integration in irregular patterns. The models of Pasupathy and Connor (1999, 2001, 2002), in representing shape as a trajectory in a curvature versus polar angle space, require all curvature features to be in specific positions in polar space relative to the pattern center. These models, however, are devised to describe suprathreshold patterns. Dickinson et al. (2013) showed in 2x2IFC experiments that an RF6 pattern with six cycles of modulation could not be discriminated from an RF6 pattern with three cycles of modulation at their threshold for detection. An implication of this result is that these patterns, near threshold, are not represented by a spatial template that requires a stimulus to match that template over its whole extent. In a recent study, however, Schmidtmann, Kennedy, Orbach, and Loffler (2012) reported that the decrease in threshold for conventional RF patterns with increasing number of cycles of modulation of a particular frequency did not conform to a power function. Instead, they claimed that the improvement conformed to probability summation until the cycle of modulation that completed that RF pattern was added and that the threshold then declined immediately to a value that implied integration of information around the pattern. Their conclusion was that the RF pattern was detected by a template mechanism that required completion of the pattern. This conclusion appears to be in conflict with the result reported in Dickinson et al. (2013), but it was, however, largely based on increment detection data in patterns with amplitudes of modulation well above detection threshold. We have not experienced such dog legs in graphs describing threshold versus numbers of cycles of modulation in data from previous studies near threshold for detection (Bell & Badcock, 2008; Dickinson, Han et al., 2010; Dickinson, McGinty et al., 2012; Tan et al., 2013), nor are they evident in Loffler et al. (2003). The irregular patterns devised for use in Experiment 3 allow us to perform a test of whether shape represen-

tation near detection threshold requires a spatial template. Experiment 4 examines whether an irregular pattern and its mirror image are perfectly discriminated. If an irregular pattern and its mirror image (which cannot be produced by simple rotation of the original) were to be discriminable at their thresholds for detection, then it might be supposed that distinct spatial templates for the two patterns exist. An inability to discriminate between the two patterns at their thresholds for detection might indicate, instead, that the patterns are globally encoded in the periodicity of their corners (specifically the set of angles subtended at the center of the pattern by adjacent points of maximum convex curvature). We find that an irregular pattern and an RF4 pattern can be discriminated at threshold for detection but that mirror images of an irregular pattern cannot. This suggests that, near threshold, it is the content of subtended angles within a pattern that defines shape rather than a template in the form of a spatial filter.

General methods

Observers

All observers were recruited from the Human Vision Laboratory of the University of Western Australia, and all gave their informed consent to their participation in the study. The study was approved by the University of Western Australia ethics committee and therefore conformed to the tenets of the Declaration of Helsinki. Three of the observers, S. C., H. R., and E. D. are authors; R. G. and T. M. were naïve to the experimental aims. All participants are experienced psychophysical observers.

Apparatus

For Experiments 1 and 2, stimuli were created using Matlab 5.3 (Mathworks, Natick, MA) installed on a PC and drawn from the frame buffer of a Cambridge Research Systems 2/3 visual stimulus generator to a Sony Trinitron G420 monitor (refresh rate 100 Hz and 1024 × 768 pixels). For Experiments 3 and 4, stimuli were created using Matlab 6.5 (Mathworks) and displayed using a Cambridge Research Systems 2/5 visual stimulus generator and a Sony Trinitron G400 monitor (refresh rate 100 Hz and 1024 × 768 pixels). The pixels of both screens subtended 1′ of visual angle at the viewing distance of 115 cm. The active area of the screens, therefore, both subtended 17.1° × 12.8°. Viewing distance was stabilized through the use of a chin rest. Background luminance of the stimuli was 45 cd/m^2 in each case, and the screens were viewed in darkened rooms with an ambient luminance of <1 cd/m^2. Luminance calibration was performed using an Optical OP200-E photometer (head model number 265) and associated software (Cambridge Research Systems). A CB3 button box was used to record responses for Experiments 1 and 2, and the computer keyboard was used for Experiments 3 and 4.

Stimuli

In all cases, stimuli were closed paths, circular or subtly deformed from circular. The paths had a nominal mean radius of 60 min of visual angle (′). Variations to this radius are detailed in the Methods sections of the experiments. The luminance profile of the patterns in radial section was the fourth derivative of a Gaussian (D4), with a spatial frequency content peaking at 8 cycles per degree of visual angle (the value of the parameter σ in equation 1 of Wilkinson et al. [1998] was 3.376′). The Weber contrast of all stimuli was 1.

Procedure

Experimental procedures either measured threshold amplitudes for detection of modulation of a single pattern type or concurrently measured threshold amplitudes for detection and discrimination of a pair of pattern types (a control condition of Experiment 2 measures thresholds for detection and discrimination in discrete blocks of trials).

In the first of the above cases, conditions were blocked. In each trial of a block, a modulated test pattern and a circular reference pattern were presented sequentially in two equal time intervals of 160 ms each and in a randomized order. Observers were required to indicate which of the two intervals, first or second, contained the test pattern. This will subsequently be referred to as a two-interval forced-choice (2IFC) experiment, and the thresholds derived will be referred to as thresholds for detection of modulation. The method of constant stimuli (MOCS) was used to derive the thresholds. Nine amplitudes of modulation of the test stimulus were employed within a block. The probability of correct response was determined for each of the nine amplitudes of modulation and the data fitted with a Quick function (Quick, 1974; Wilson, 1980). The Quick function is given by

$$p(A) = 1 - 2^{-\left[1+(A/\Delta)^{Q}\right]} \quad (1)$$

where A is the modulation amplitude as a proportion of the radius of the unmodulated circle, Δ is the threshold at the 75% correct performance level, and Q is a measure of the slope of the psychometric function.

In the second of the two cases, trials incorporating two different patterns were interleaved within a block. Each trial again consisted of a test pattern and reference pattern presented in different intervals. Observers were required to respond twice for each trial. The first response was to indicate which of the two intervals contained the test stimulus, detection of modulation, and the second response was to indicate which of the two different test patterns was present in that trial, identification. This paradigm will be referred to as a two-decision, two-interval, forced-choice (2x2IFC) experiment. Nine amplitudes of modulation were used for each of the two types of test pattern present in each condition. The responses pertaining to the detection and identification of the two test patterns were collated; probabilities for the correct first and second response for each stimulus type were calculated for all amplitudes of modulation. Where required, amplitudes were normalized to equate the angular deviation from circular across pattern types, and the probabilities of correct performance were then seen to be equal across pattern types. Quick functions were fitted to data collapsed across pattern types. The fitted parameters of the Quick functions yielded the amplitude thresholds for 75% correct performance in detection and discrimination of the two different stimuli and also measures of the slopes of the psychometric functions.

Experiment 1: Information is integrated around patterns deformed from circular by positively and negatively rectified sinusoidal modulation of radius

Introduction

Experiment 1 examined the amplitude thresholds for detection of modulation in conventional RF patterns and negatively and positively full-wave rectified RF patterns. The potential for integration in positively and negatively rectified RF stimuli has not previously been examined, and the implications of changes in the local orientation and curvature properties of these stimuli are explored. Using a 2IFC experimental paradigm, the thresholds for detection of modulation in patterns with the same frequency but different numbers of cycles of modulation were measured to determine whether the global integration of information, previously demonstrated in conventional RF patterns, is also seen for rectified patterns. Rectification of the sinusoidal modulation present in RF patterns results in patterns that have double the periodicity. At threshold, RF patterns have the same number of points of maximum curvature as cycles of modulation, and these points are all convex on the shape. Therefore, for the purposes of our experiment investigating the analysis of shape in the visual system, the frequency of modulation was halved before rectification to create patterns with the same number of points of maximum convex curvature. The one model proposed to explain sensitivity to RF patterns (Poirier & Wilson, 2006) uses a continuous measure of curvature around the points of maximum curvature. Rectification of the sinusoidal modulation produces patterns that have substantially different curvatures at these points and can, therefore, be expected to be a robust test of whether a continuous measure of curvature is necessary for integration of shape information in the visual analysis of RF patterns. Also of interest is whether positively rectified patterns, which contain points where the boundary is concave, are compromised in their integrations with respect to the negatively rectified patterns, which do not contain such points. This might be expected because it has been argued that complex patterns might be deconstructed by parsing of the pattern at matched concavities (Biederman & Cooper, 1991; Hoffman & Richards, 1984). For the conventional and negatively rectified patterns, the curvature is always positive for the amplitudes shown here (and for all experimental amplitudes used) because of the constant background curvature of the unmodulated circular path.

Methods

Stimuli

The test stimuli were conventional RF patterns (Loffler et al., 2003; Wilkinson et al., 1998) and positively and negatively rectified RF patterns. The conventional RF patterns (denoted *RF* in figures) had a sinusoidally modulated radius given, as a function of polar angle, by Equation 2.

$$R(\theta) = R_0\left(1 + A\sin(\omega\theta + \phi)\right) \quad (2)$$

where θ is the angle made with the x-axis, R_0 the mean radius, A the amplitude of modulation, ω the frequency of modulation (cycles in 2π radians), and ϕ the phase of the modulation (all patterns were presented in random phase). The radius of the positively rectified stimuli (denoted +ve) is given by

$$R(\theta) = R_0\left(1 - A + abs\left(A\sin\left(\frac{\omega}{2}\theta + \phi\right)\right)\right) \quad (3)$$

and the negatively rectified stimuli (denoted –ve) by

$$R(\theta) = R_0\left(1 + A - abs\left(A\sin\left(\frac{\omega}{2}\theta + \phi\right)\right)\right) \quad (4)$$

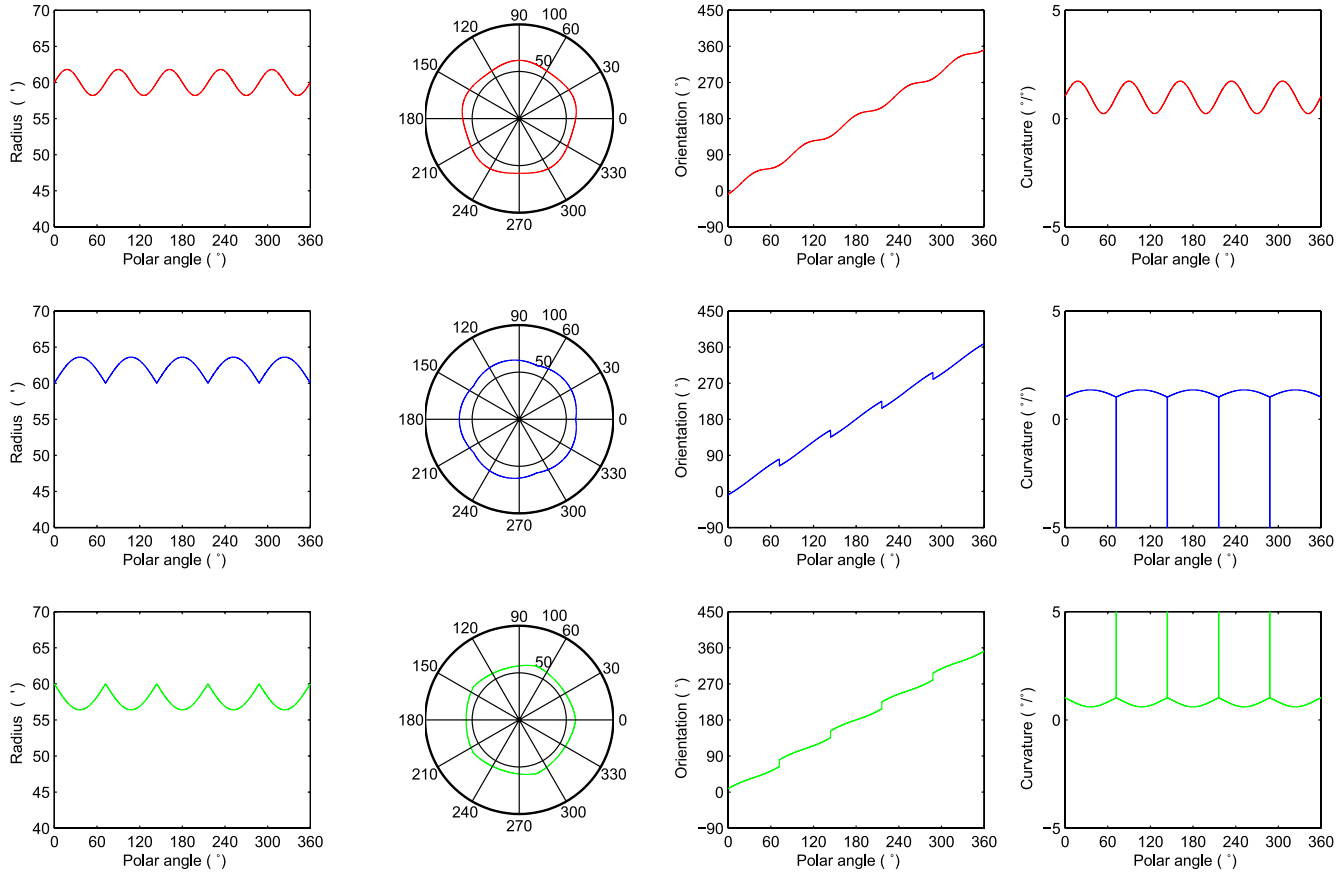

Figure 1. An illustration of the stimuli used in Experiments 1 and 2. The three rows of graphs illustrate properties of the three different types of stimuli used. The first row describes a conventional RF pattern with five cycles of modulation in 2π radians, commonly referred to as an RF5 pattern. The second and third describe patterns created using positively and negatively rectified sinusoids with 2.5 cycles of rectified sinusoidal modulation in 2π radians, respectively. The period of the waveform of the modulation is therefore the same across all stimulus types, and all patterns contain the same number of points of maximum convex curvature. The amplitude, *A*, of the RF5 pattern is 0.03, and the amplitudes of the rectified patterns are 0.06 (amplitude is expressed as a proportion of the circular radius R_0). The patterns, therefore, all have the same peak-to-peak amplitude. The left-hand column of graphs shows how the radii of the stimuli vary with polar angle, and the closed paths in the polar plots (colored lines) show the form of the patterns exhibiting this modulation of radius (the circular grid lines of the polar plot represent radii of 50 and 100 min of visual angle). The third column shows how orientation in a Cartesian frame of reference varies with polar angle and the fourth the rate of change of this angle with respect to polar angle (a positive rate of change indicates a counterclockwise rotation with increase in polar angle). It can be seen that the conventional RF pattern is characterized by a smooth change in curvature whereas the two rectified patterns contain points of mathematically infinite curvature (discontinuities in orientation).

The frequency of the sinusoidal modulation is halved before rectification to create patterns with the same number of points of maximum convex curvature. The orientation of the conventional RF path expressed as a function of θ is given by

$$\alpha(\theta) = \tan^{-1}\left(\frac{A\omega\cos(\omega\theta+\phi)}{R(\theta)/R_0}\right) + \theta \qquad (5)$$

where for the angle α, the value zero is defined to correspond to vertical. The orientations for the rectified patterns are also derived from this function with the appropriate modifications of frequency, amplitude, and sign. The value for R_0, nominally 60 min of visual angle, was allowed to vary by $\pm 5\%$, at random to preclude the use of average pattern radius as a reliable cue to pattern identity, and the pattern center allowed to move $\pm$ one eighth of the pattern radius in the horizontal and vertical dimensions to prevent the buildup of afterimages that might be used as references and also to prevent the edges of the screen being used as alternative cues to shape change.

Illustrations of the three types of stimuli are presented in Figure 1. For the illustrations, $\phi = 0$. The curvature measure was calculated numerically as the rate of change of orientation with polar angle. For the small amplitudes of modulation used, the path length for one radian of polar angle approximates the radius

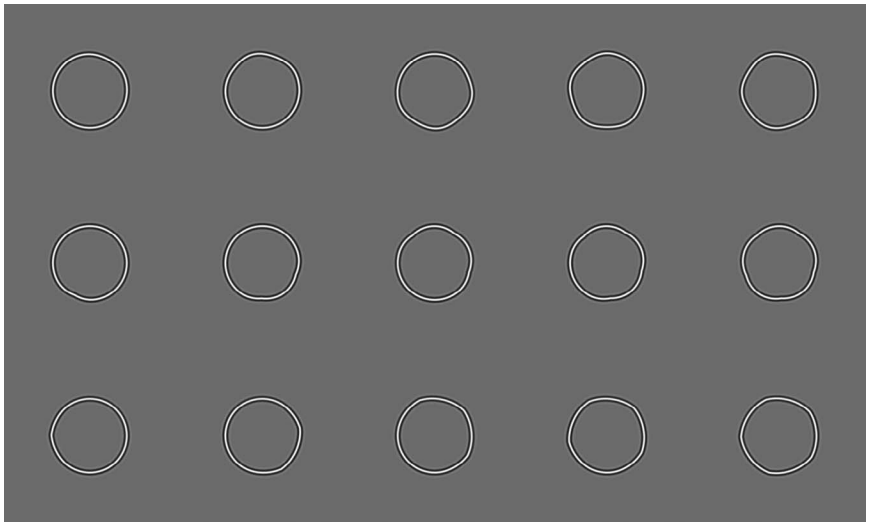

Figure 2. Example stimuli. The example stimuli in the five columns have one, two, three, four, and five cycles of modulation left to right. The stimuli of the top row are conventional RF patterns and the second and third rows positively and negatively rectified patterns, respectively. The patterns are presented in random phase as they were in the experiment and have equal peak-to-peak amplitude of modulation.

of the pattern. Curvature in the Cartesian frame, the rate of change of orientation with path length, scales in inverse proportion to size. Thus, when considering patterns of a fixed size, comparison of local curvature when expressed as rate of change of orientation with path length, is, other than a change of unit, equivalent to the comparison of curvature expressed as the rate of change of orientation with theta.

The illustrations of the stimuli presented in Figure 1 all have five cycles of modulation. Figure 2 shows example stimuli of the three types with one, two, three, four, and five cycles of modulation. The rectified stimuli have amplitudes of 0.05 and the unrectified patterns 0.025. For conventional RF5 patterns, this amplitude is approximately 10 times the threshold for detection and for one cycle 2 to 3 times detection threshold. All types of stimuli were devised in such a way as to avoid introducing discontinuities in orientation at the end of the trains of modulation in patterns that do not have the full complement of five cycles of modulation. The conventional RF patterns had half cycles of sinusoidal modulation at the ends of the trains of modulation replaced by the corresponding halves of a first derivative of a Gaussian (D1) function with the same amplitude and maximum value for the first derivative (Loffler et al., 2003). The trains of modulation in the rectified stimuli were ended at maxima of the sinusoidal modulation, points at which the function was tangent to the circular remainder of the path (cf. Equations 3 and 4).

Procedure

The 15 experimental conditions represented by the 15 stimuli shown in Figure 2 were blocked. The conditions were examined independently in separate blocks of trials. In each trial of a block, a modulated test pattern and a circular reference pattern were presented sequentially in two equal time intervals of 160 ms each and in a randomized order. Observers were required to indicate which of the two intervals, first or second, contained the test pattern, a 2IFC task. For each condition, 20 trials at each of the nine amplitudes of modulation used in the MOCS were performed in each of three blocks. Every psychometric function, therefore, incorporated the responses to 540 trials. The Quick function fitted to the psychometric data for each condition yielded the amplitude at which the observer performed at the 75% correct level (Δ) and a measure of the slope of the psychometric function (Q).

Results

Thresholds were measured for patterns with one, two, three, four, and five cycles of sinusoidal and positively and negatively rectified sinusoidal modulation for five observers. The results are presented in Figure 3. The functions describing the decrease in threshold with increasing number of cycles of modulation are power functions (straight lines on log-log graphs) for all three types of stimuli. Thresholds for the conventional RF patterns are represented by red circles, and the fitted function is described by a solid red line. The data and functions pertaining to the stimuli with positively and negatively rectified sinusoidal modulation are rendered in blue and green, respectively. The power function fits yielded indices for the power functions that represented the rate of decrease of

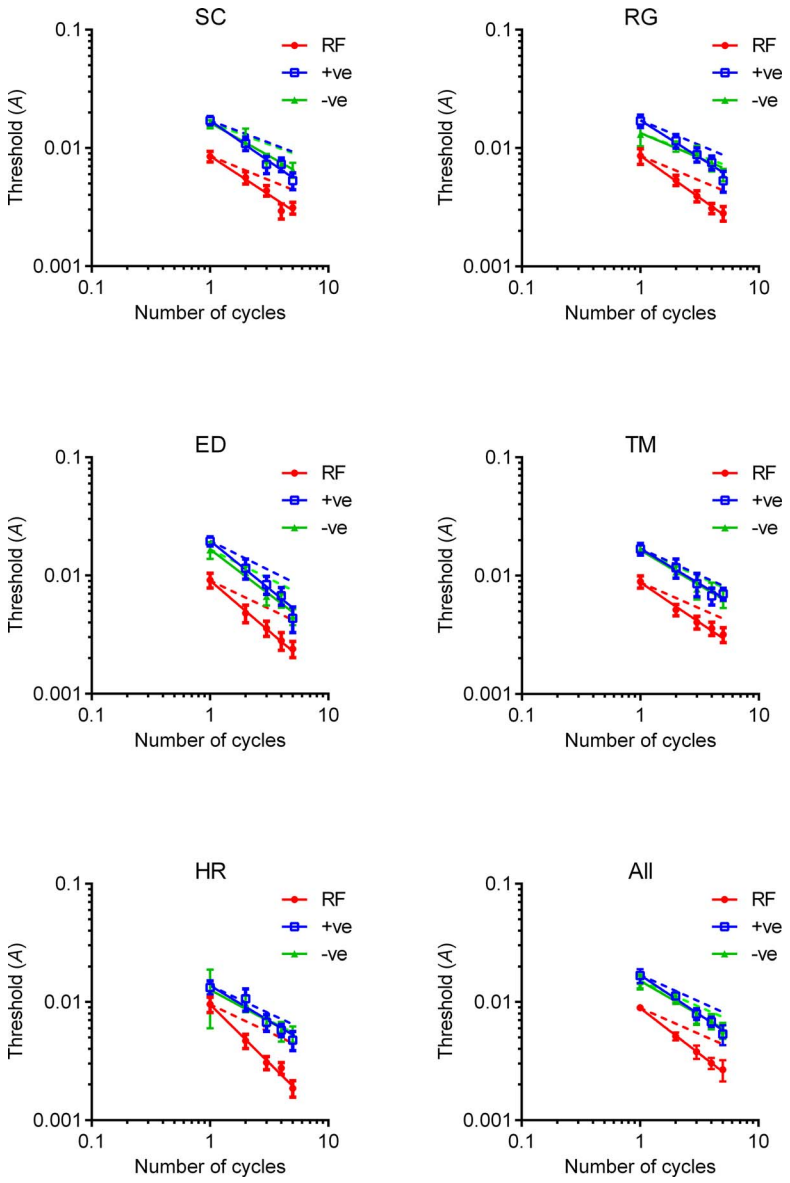

Figure 3. Thresholds for the detection of modulation in the three pattern types. Thresholds are plotted against number of cycles of modulation on the patterns. Data pertaining to conventional RF patterns are in red, positively rectified patterns in blue, and negatively rectified patterns in green. Error bars are 95% confidence intervals. The data are fitted by power functions. Functions predicted by probability summation are plotted as dashed lines.

thresholds with increasing numbers of cycles of modulation. Integration of information is implied by a rate of decrease in threshold with number of cycles of modulation that exceeds that which can be attributed to probability summation, the improved probability of detecting single cycles as the number of cycles present is increased. The index of the power function that would be predicted for probability summation can be derived from the parameter Q that describes the steepness of the Quick functions fitted to the psychometric data (Loffler et al., 2003; Quick, 1974; Wilson, 1980). The probability summation prediction for the index is given by $-1/Q$ (see Equation 1). For each of the three types of stimulus, the observed indices were compared with the indices predicted for probability summation in paired, one-tailed t tests for the population of observers. The rate of decrease in threshold with increase in the number of cycles of modulation was found to be significantly steeper than that predicted by probability summation for RF patterns, $t(4) = 6.460$, $p = 0.0015$; positively rectified patterns, $t(4) = 5.208$, $p = 0.0032$; and negatively rectified patterns, $t(4) = 2.910$, $p = 0.0218$. Individual values for the indices and the means are presented in Table 1. Functions predicted by probability summation are plotted as dashed lines in Figure 3.

Observer	RF5		+ve		−ve	
	$\gamma(1-5)$	$-\frac{1}{Q}(1-5)$	$\gamma(1-5)$	$-\frac{1}{Q}(1-5)$	$\gamma(1-5)$	$-\frac{1}{Q}(1-5)$
SC	−0.66	−0.41	−0.70	−0.38	−0.56	−0.37
ED	−0.86	−0.48	−0.81	−0.50	−0.76	−0.50
HR	−0.99	−0.47	−0.60	−0.49	−0.54	−0.52
RG	−0.71	−0.42	−0.63	−0.42	−0.42	−0.38
TM	−0.68	−0.44	−0.60	−0.45	−0.60	−0.45
All	−0.78 (0.18)	−0.44 (0.04)	−0.67 (0.11)	−0.45 (0.06)	−0.58 (0.15)	−0.44 (0.09)
	$\gamma(2-5)$	$-\frac{1}{Q}(2-5)$	$\gamma(2-5)$	$-\frac{1}{Q}(2-5)$	$\gamma(2-5)$	$-\frac{1}{Q}(2-5)$
SC	−0.75	−0.42	−0.73	−0.45	−0.79	−0.38
ED	−0.76	−0.48	−0.92	−0.53	−0.91	−0.50
HR	−0.92	−0.47	−0.91	−0.51	−0.71	−0.49
RG	−0.74	−0.43	−0.74	−0.44	−0.56	−0.36
TM	−0.53	−0.45	−0.65	−0.49	−0.52	−0.47
All	−0.74 (0.17)	−0.45 (0.03)	−0.79 (0.15)	−0.48 (0.05)	−0.70 (0.20)	−0.44 (0.08)

Table 1. Indices of the power functions describing thresholds as number of cycles of modulation is increased. *Notes:* For RF5, positively (+ve) and negatively (−ve) rectified patterns of the indices of the power functions, γ, are compared with the predictions of probability summation, $-1/Q$, for fits to the thresholds for one to five and two to five cycles of modulation. Indices of fits to the data are seen to be systematically larger in magnitude than the probability summation predictions, suggesting integration of shape information across cycles of modulation.

It is evident from Figure 3 that the thresholds for detection of the positively and negatively rectified patterns are about twice those for conventional RF patterns with the same number of cycles of modulation. In fact the geometric mean of the ratio of thresholds for positively rectified patterns and conventional RF patterns across the observers is 2.08 ± 0.12 (95% confidence interval), for stimuli paired by number of cycles of modulation. For negatively rectified patterns it is 2.03 ± 0.13. This ratio of two in thresholds defined by the amplitude parameter A (see Equations 2, 3, and 4) between rectified and conventional RF detection thresholds results in equal peak-to-peak amplitudes.

Although the data were consistent with integration of shape information around all of the patterns, there is some suggestion, particularly evident in the data of H.R., that the thresholds for the single-cycle conditions were lower than expected for the rectified patterns, particularly the negatively rectified pattern. Table 1 shows the indices of the power functions fitted in Figure 3 and also power functions fitted to the threshold for two to five cycles of modulation. Also tabulated for comparison are the probability summation predictions for the indices of the power functions, given by $-1/Q$, where Q is the average of the slopes of the Quick functions fitted to the probabilities of correct response in the 2IFC detection of modulation task. If the single-cycle conditions are excluded, then the indices of the power functions are very similar across the three conditions. A one-way repeated-measures analysis of variance comparing the indices obtained for one to five cycles showed that there was an effect of condition, $F(2, 8) = 5.188$, $p = 0.0359$, and Tukey's multiple comparison test indicated that this was due to a significant difference between the indices for the conventional RF patterns and the negatively rectified condition, $q(8) = 4.546$. The same analysis for the indices considering the data only for two to five cycles showed no effect of condition, $F(2, 8) = 1.473$, $p = 0.2854$, and Tukey's multiple comparison test confirmed there was no significant difference in any pairwise comparison. This result indicates that there were no statistically significant differences between stimulus types in the efficiency of integration of information across cycles if the single-cycle thresholds (which cannot include integration across cycles) were excluded.

An explanation for this particular observation is that, for the higher amplitude single-cycle patterns, a salient local cue to the existence of modulation is present that is not integrated across cycles of modulation. It is plausible that this cue might be the point of infinite curvature (discontinuity in orientation) and that the global pattern becomes more salient as cycles of modulation are added because of the integration of the global cue to shape and the absence of integration in the cue that is most salient in a higher amplitude single-cycle pattern.

Discussion

The results of Experiment 1 demonstrate that integration of modulation information occurs in all three types of pattern. Given that discontinuities in orientation (points of infinite curvature) exist on both the positively and negatively rectified patterns, we can conclude that the existence of such points on the

patterns does not disrupt the global processing of information around the patterns.

Experiment 1 also shows that the thresholds for the rectified patterns are twice those for the conventional RF patterns. At threshold, then, the different patterns have the same peak-to-peak amplitudes. When the patterns have the same peak-to-peak amplitude, they have different curvatures but have the same orientation content with respect to circular (that is, they have the same histogram of orientations if orientation is defined as a local deviation from circular). The distribution of the positions of the points of maximum orientation difference from circular is, however, different, and this leaves open the possibility that the patterns may appear to be different. Subjectively, though, the shapes of the patterns appear to be defined by a fivefold rotational symmetry. Experiment 2 investigates the degree to which the patterns can be discriminated near their thresholds for detection. Evidence that the patterns cannot be discriminated at their thresholds for detection might suggest that local information has been discarded in the formation of an economic representation of shape, based on the relative positions of points of maximum convex curvature that are identical across the pattern types.

Experiment 2: Conventional RF patterns and positively and negatively rectified RF patterns are not discriminable at their thresholds for detection

Introduction

Dickinson et al. (2013) showed that RF3 and RF6 patterns can be discriminated at their thresholds for detection. This was also true for patterns that had two cycles of modulation each but not for patterns with a single cycle. This result was taken to indicate that the critical feature that renders RF patterns discriminable is the angle subtended at the center of the pattern by adjacent points of maximum convex curvature. It is interesting to note that the points of maximum curvature and the points of maximum deviation from circular are not coincident across the three pattern types (see Figure 1). They are coincident for the negatively rectified patterns but are maximally separated for the positively rectified patterns. For conventional RF patterns, with low amplitudes of modulation, the points of maximum deviation from circularity are close to the zero crossing of the sinusoidal modulator (Dickinson, McGinty et al., 2012; Mullen, Beaudot, & Ivanov, 2011) and therefore are situated at points $\pm\pi/2$ radians from the maxima on the sinusoid. The curvature defined as the rate of change of orientation in the Cartesian reference frame with polar angle at these points is the same as a circular arc at the same radius (although the measure of curvature employed in the Poirier and Wilson [2006] model is zero at these points, being defined as the curvature difference from this arc). Thus, we arrive at the seemingly paradoxical position that the threshold for detection of modulation in RF patterns is limited by the maximum angular deviation from circularity (although this maximum deviation does not remain constant as cycles are added as might be claimed by Mullen, et al. [2011] but declines), but shape is encoded in the relative positions of maximum convex curvature. Moreover, the results of Experiment 1 imply that orientation difference from circular predominates over curvature in determining the salience of modulation for rectified patterns as well as the conventional patterns. This raises the possibility that the positions of the points of maximum curvature are determined by detectors exploiting the maximum deviation from circularity on the shoulders of the points of maximum curvature. The indifference to the positions of these points of maximum curvature to the efficiency of integration suggests that this information is not retained in the shape representation of these patterns near their thresholds for detection. If the angle at such points were not encoded at threshold for detection of the modulation, then the patterns would be indistinguishable at this threshold. Demonstration that the three pattern types are not discriminable at their thresholds for detection might therefore indicate that in the formation of an economic shape representation, the local information used in the analysis is discarded. Lennie (1998) refers to this as a *perceptual decision* in the hierarchical analysis of shape.

Experiment 2, then, measured thresholds for detection and discrimination of the three types of pattern modulation used in Experiment 1 in a 2x2IFC experiment. All three pattern types have a fivefold symmetry, but the distribution of local radii, orientations, and curvatures differs substantially across the patterns. If the patterns were encoded by a continuous measure of any one of these properties in spatial templates that required stimuli to match templates over the whole of their extent, one might expect the patterns to be discriminable at their thresholds for detection.

Methods

Stimuli

The stimuli were patterns of the three types used in Experiment 1, modulated around the whole pattern (see Figure 1 for schematics and the right-hand column of Figure 2 for example stimuli).

Procedure

The three types of patterns were paired in separate blocks. In a 2x2IFC experiment, thresholds for detection and identification of the patterns were measured using the MOCS. For each pair of stimulus types (for example, a conventional RF pattern and a negatively rectified RF pattern), nine amplitudes of modulation of each of the pair of patterns was used with 20 trials at each amplitude performed in three blocks of trials, a total of 540 trials for each psychometric function. For each trial, the observer was required to indicate, in successive responses, which of the two intervals contained the modulated test stimulus and which stimulus of the pair of possible stimuli it was. The responses were collated within amplitudes and the probabilities of correct performance calculated. For this experiment, the amplitudes used were peak-to-peak amplitudes rather than the amplitude of maximum radial deviation from circular specified by the parameter A used in Equations 2–5. Each of the three pattern types has the same maximum orientation difference from circular and the same orientation histogram when they have the same peak-to-peak amplitude. Under these circumstances, as demonstrated in Experiment 1, the different patterns have the same salience. Quick functions were therefore fitted to the detection and identification data across the pattern types of each pair to compare thresholds for detection and discrimination of the patterns (see Figure 4). Because the responses were ordered (i.e., detection first response and discrimination second), potentially leading to an overestimate in sensitivity to one or other of the tasks, a control experiment was performed for which detection and discrimination tasks were completed in separate blocks. Three of the four observers completed one each of the stimulus pairings.

Results

The psychometric data and fitted Quick functions for the three pairs of stimulus types and four observers are shown in Figure 4. The probabilities of correct response are plotted against the full amplitude. That is the amplitude A for the RF stimuli and $2A$ for the rectified stimuli. To confirm that the patterns had the same salience at the same peak-to-peak amplitudes, the data were combined across the block to derive detection thresholds for each pattern type. The mean thresholds for detection of peak-to-peak modulation are 0.00506 $\pm$ 0.00087 (95% confidence intervals), 0.00582 $\pm$ 0.00116, and 0.00526 $\pm$ 0.00121 for the conventional RF and positively rectified and negatively rectified RF stimuli, respectively. Paired, two-tailed t tests of the thresholds across the pairs RF/+ve, RF/−ve, and +ve/−ve showed that the thresholds were not significantly different, $t(3) = 2.709$, $p = 0.0733$; $t(3) = 1.332$, $p = 0.2749$; and $t(3) = 1.446$, $p = 0.2438$, respectively, when thresholds were expressed as peak-to-peak amplitudes. Given this result, the two sets of data for detection for each pair of stimuli within a block were combined, as were the thresholds for identification, for the comparison of thresholds for detection and discrimination of the pattern types.

The solid black lines representing fitted functions in Figure 4 are the best-fitting Quick functions for the combined detection data for pairs of patterns, and the dashed black lines represent the Quick functions fitted to the combined identification data. If the patterns could be individually identified at their thresholds for detection, then these lines would be coincident. Obviously, the patterns cannot be discriminated at their thresholds for detection. Table A1 of the Appendix reports extra sum of squares F tests (GraphPad Prism version 6.01 for Windows, GraphPad Software, San Diego CA, www.graphpad.com) comparing the functions fitted to the detection and identification data.[1]

Figure 5 shows the results of the control experiment performed to investigate the effect of the added demand of making two responses to each trial in the 2x2IFC experimental paradigm. The probabilities for correct detection and identification, plotted against peak-to-peak amplitude, displayed in Figure 5 were determined using a single-response 2IFC experimental paradigm. The detection and identification thresholds were therefore measured in separate blocks of trials. For comparison, the fits to the pertinent detection and identification data measured in the 2x2IFC experiment displayed in Figure 4 are plotted as gray solid and dashed lines, respectively. The results demonstrate that there is no systematic difference across the two experimental paradigms. The functions represented by the solid and dashed black lines are used to compare performance in the detection and identification of the pairs of pattern types. For the three observers, independent fits to the detection and identification data were preferred to the null hypothesis of a global fit: ED, $F(2, 104) = 70.00$, $p < 0.0001$; SC, $F(2, 104) = 64.65$, $p < 0.0001$; TM, $F(2, 104) = 61.55$, $p < 0.0001$.

Discussion

Experiment 2 measured probabilities of correct performance in the detection and identification of conventional and positively and negatively rectified RF patterns. Near their detection and discrimination thresholds, all three patterns are characterized by the possession of five points of maximum curvature and a fivefold rotational symmetry. They do, however, differ substantially in the distribution of modulation amplitude, local Cartesian orientation, and curvature. The

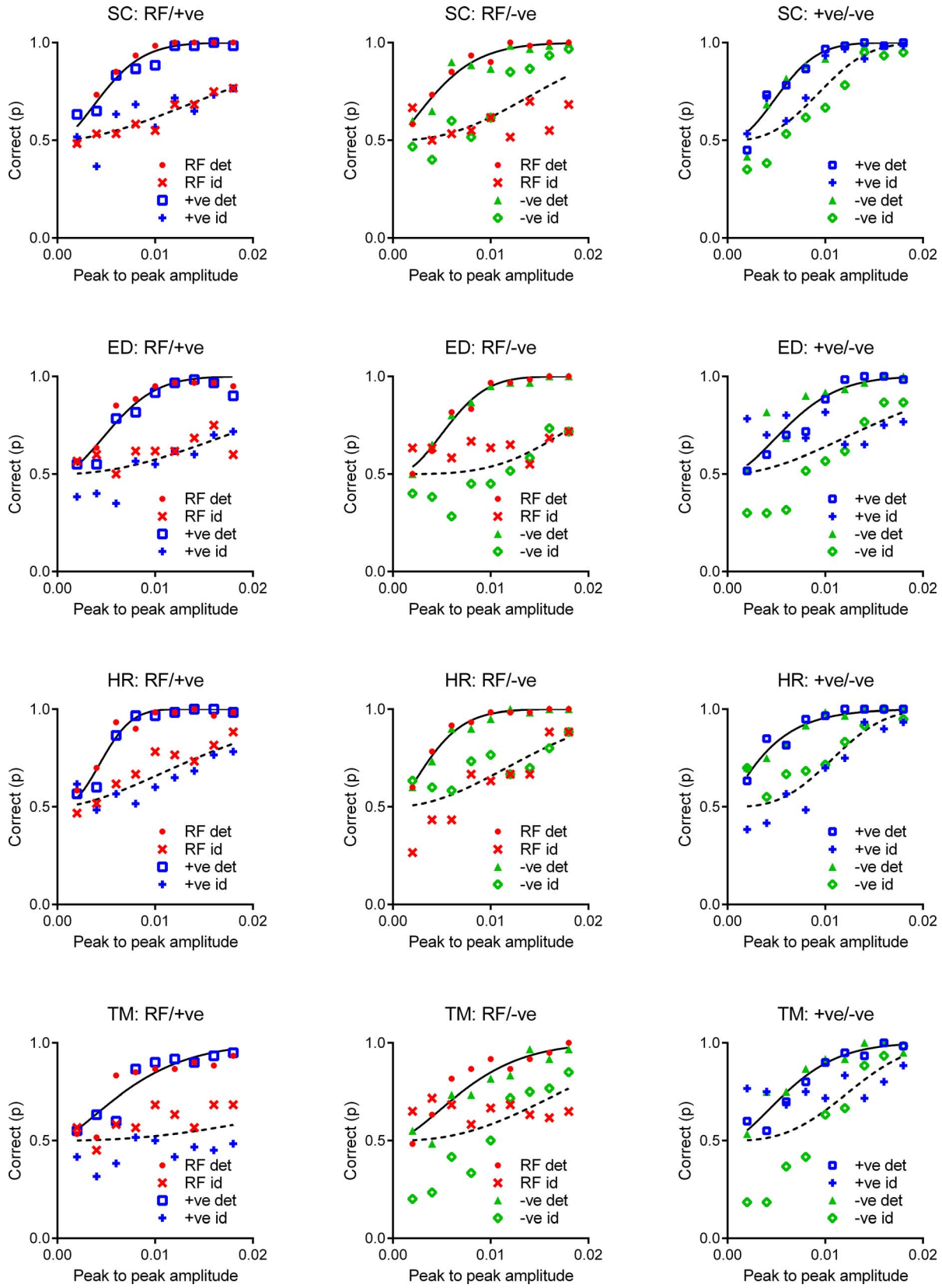

Figure 4. Psychometric data describing performance in detection of modulation and identification of pattern type. Performance is measured as the probability of correct response as a function of peak-to-peak modulation amplitude. Data pertaining to the RF patterns is presented in red, positively rectified patterns in blue, and negatively rectified patterns in green (following the convention

→

←

of Figures 1 and 3). Detection data are represented by red dots, open blue squares, and filled green triangles. Identification data are represented by red crosses, open green diamonds, and blue plus symbols. The solid black lines represent Quick functions fitted to the detection data of each pair of patterns and the dashed black lines Quick functions fitted to the identification data for the pair of patterns. The functions represented by the solid and dashed black lines are used to compare performance in the detection and discrimination of the pairs of pattern types.

experiment demonstrated that the patterns could not be discriminated at their thresholds for detection. This result indicates that the distributions of modulation amplitude, Cartesian orientation, and curvature around the patterns are not critical to the encoding of the shapes by the visual system. At threshold, however, the maximum orientation difference from circular was consistent with being equal for the three patterns, indicating that this property of the patterns might limit threshold. These points are distributed differently around the pattern types, yet the patterns were not discriminable at their thresholds for detection. The points of maximum orientation difference from circular are also points at which the path is closer to linear in Cartesian space than at or around the points of maximum curvature. Such points would, therefore, more strongly stimulate the linear spatial filters of the primary visual cortex. For these patterns, pairs of these points are symmetrically arranged around points of maximum curvature on the path and might be expected to encode such points as angles. This result is then consistent with the encoding of shape by the angles subtended by adjacent corners on the patterns, proposed by Dickinson et al. (2013). If this conclusion is drawn, discrimination between the pattern types must be performed on the basis of local information at higher amplitudes of modulation. Close scrutiny of Figure 4 reveals that performance in the identification of positively and negatively rectified patterns is enhanced when these stimuli are paired. It might be speculated, then, that a preferred local cue might be a local measure of convex curvature that is maximally different across these two stimuli.

Experiment 3: RF patterns incorporating cycles of modulation with differing periods, irregular RF patterns, are globally analyzed by the visual system

Introduction

The thresholds for detection of modulation in patterns derived in Experiments 1 and 2 for the three pattern types are equal if amplitudes of modulation are measured peak to peak. The significance of this result can be appreciated by considering the relationships between the modulation of radius, orientation, and curvature in RF patterns with respect to the radius, orientation, and curvature of a circle. The modulation of the radius of a pattern (in zero sine phase) is sinusoidal:

$$A_\theta = A\sin(\omega\theta) \quad (6)$$

where A_θ is the amplitude at an angle θ and ω is the RF.

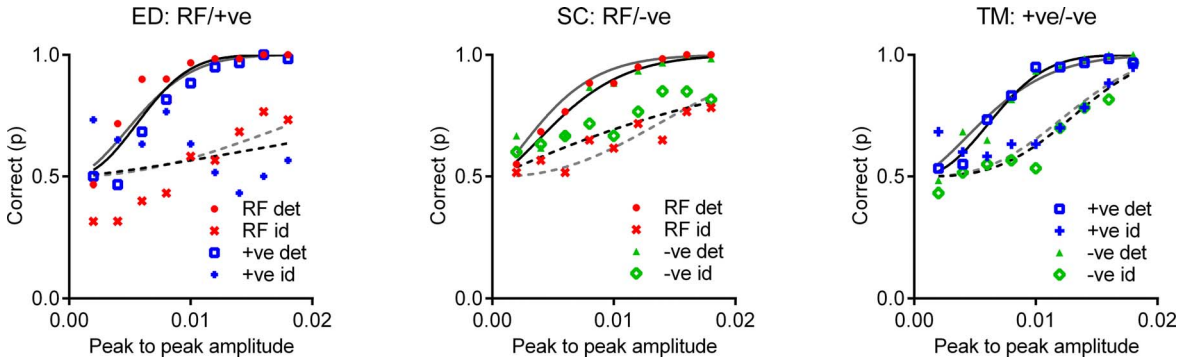

Figure 5. A comparison of data gathered using a 2IFC experimental paradigm with the data previously collected using a 2x2IFC paradigm. The psychometric data describing performance in detection of modulation and identification of pattern type shown above were collected in independent blocks of trials rather than two responses to the same trial. The solid black lines represent Quick functions fitted to the detection data of each pair of patterns, and the dashed black lines Quick functions fitted to the identification data for the pair of patterns.

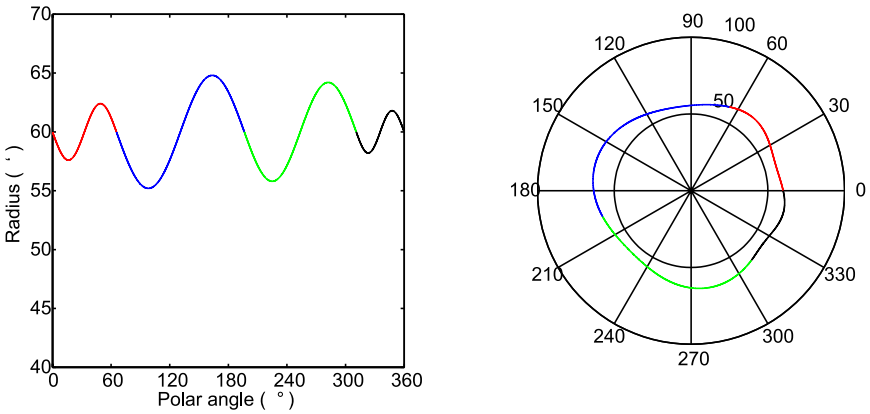

Figure 6. An illustration of the irregular RF patterns used in Experiments 3 and 4. The pattern is composed of a single cycle each of modulation with radial frequencies of 22/4 (red), 22/8 (blue), 22/7 (green), and 22/3 (black). The amplitude of the cycle with the radial frequency of 22/4 is 0.04. The amplitudes of the other cycles are scaled by the ratio of their periods to the period of this first cycle.

The gradient of this function is given by the first derivative with respect to θ:

$$\frac{dA_\theta}{d\theta} = A\omega\cos(\omega\theta) \quad (7)$$

and, for the small angles of departure from circular at detection thresholds, the orientation with respect to circular varies approximately linearly with the first derivative. The curvature, expressed as the rate of change of orientation with respect to circular, is therefore proportional to the second derivative of the modulation in radius:

$$\frac{d^2A_\theta}{d\theta^2} = -A\omega^2\sin(\omega\theta) \quad (8)$$

When the RF pattern is rectified the rectified, parts of the pattern retain the same magnitude of orientation difference from circular, but the sign of the angles changes. The rectified patterns, however, have half the period of the RF pattern (a useful measure of the period is the angular distance between peaks on the waveforms). Stretching the waveform such that the peak-to-peak distance is doubled, to restore the frequency of repetition of the local features of the pattern (for example, the peaks), halves the magnitudes of the angular differences from circular. If, upon rectification, the modulation amplitude is doubled when the period is doubled, then the rectified patterns have the same content of orientation difference from circular as the original RF pattern. The distribution of that orientation content is, however, changed. Orientation discontinuities are introduced, creating points of infinite curvature (angles). That the detection thresholds equate when expressed as peak-to-peak amplitudes suggests, therefore, that it might be the content of orientation difference from circular that limits performance in the detection of modulation in the patterns.

Dickinson et al. (2012) showed that thresholds of RF patterns with the same number of cycles but different frequencies of modulation were inversely proportional to the frequency of the patterns. If maximum amplitude of modulation was the critical property, then, by definition, the thresholds would be independent of frequency. If the critical property was curvature, then we can see from Equation 8 that thresholds would be expected to be inversely proportional to the square of the frequency. As well as providing important constraints on the models of analysis of RF patterns in the visual system, this information also allows us to construct irregular patterns with cycles of modulation that are equally salient. Single cycles of sinusoidal modulation that are scaled by the inverse of their frequencies are equally salient and have the same magnitude of orientation with respect to circular at their zero crossings. Such cycles of modulation can therefore be smoothly concatenated. This experiment examines whether patterns created in this way are globally integrated. If the patterns are globally integrated, this would show that the mechanism that performs the integration does not require a constant frequency of modulation, sinusoidal or otherwise, around the pattern and move the analysis of shape coding toward more complex bounding shapes.

Methods

Stimuli

Irregular patterns were created by concatenating cycles of sinusoidal modulation with different frequencies. The frequencies used were 22/4, 22/8, 22/7, and 22/3 cycles of modulation in 2π radians. An illustration of how the stimulus was composed is shown in Figure 6. The amplitude quoted in the results for the irregular pattern is the amplitude of the pattern with a

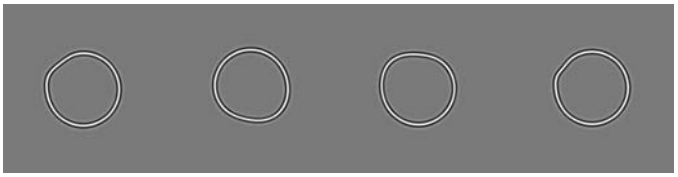

Figure 7. Examples of single-cycle RF pattern stimuli. These patterns have amplitudes normalized to an amplitude of 0.04 in the pattern with a frequency of 22/4.

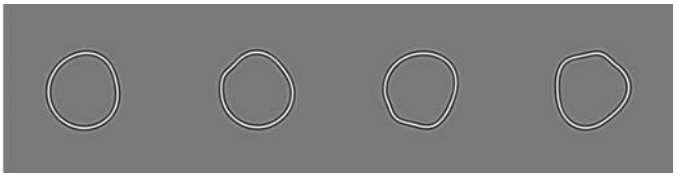

Figure 8. Example irregular stimuli with one, two, three, and four cycles of modulation. These patterns have amplitudes normalized to 0.04 (0.04 for a pattern with a frequency of 22/4). Note that from left to right, the modulation on the pattern becomes more apparent as increasing numbers of cycles of modulation are added.

frequency of 22/4 cycles per 2π radians, with the amplitudes of each of the other frequencies scaled by the inverse of the ratio between their frequency and 22/4 (for example, when the amplitude of the cycle with frequency of 22/4 is 0.04, the amplitude of the cycle with a frequency of 22/8 is 0.08). The cycles with differing frequencies of modulation were joined smoothly at the zero crossing of the sinusoid. For the low amplitudes of modulation used in this experiment, the maximum deviation of orientation from circular is coincident with this point (Dickinson, McGinty et al., 2012). The radius of the pattern changes with frequency due to the scaling process used to equate the first derivatives at the zero crossings (see Equation 7), and if the constant circular curvature is removed, the curvature scales with an additional factor of frequency (see Equation 8). The radius of higher-frequency cycles is lower and the curvature of higher-frequency patterns is higher. To reiterate, the maximum orientation difference remains constant, the maximum radius decreases with frequency, and the maximum curvature increases with frequency.

These particular irregular patterns are handed in the sense that a mirror image of the pattern cannot be superimposed on the original simply by rotation. In Experiment 4, we exploit this property and so examine if both the original and its mirror image display integration of information, and to ensure that the observers have similar exposure to the original pattern and its mirror image, both were tested using the same procedure.

Procedure

Thresholds for patterns with one, two, three, and four cycles of modulation were measured using a 2IFC task and the MOCS. Conditions defined by the number of cycles of modulation were blocked. Each block comprised 360 trials in which the observer was required to report which of two patterns presented was the modulated test pattern. The other pattern was a circular reference pattern. Patterns were randomly positioned within a 6′ range in the vertical and horizontal, a substantial range of variation relative to the modulation detection threshold.

For the single-cycle condition, the single cycle of sinusoidal modulation was replaced by a D1 with the same amplitude and maximum value for the first derivative (Loffler et al., 2003). Each frequency (see Figure 7) was presented in a quarter of trials of the block across nine different amplitudes. Examples of one-, two-, three-, and four-cycle conditions of the original pattern are presented in Figure 8. For the two-(three-) cycle condition, each of the four possible pairs (triples) of contiguous cycles were presented in a quarter of the trials. and the first and last half cycles of the train of cycles of modulation were replaced by the two halves of the appropriate D1 function. For the four-cycle condition, the complete pattern was presented in all trials. Three blocks of trials were performed for each condition. To verify that the single cycles of modulation were all equally salient at their normalized amplitudes, the results of the trials pertaining to each particular frequency of modulation were collated and the probabilities of correct response for each of the four frequencies fitted independently by the Quick function. The individually determined thresholds for the single-cycle stimuli are presented in Figure 9. Because the thresholds did not differ, the psychometric data were subsequently amalgamated for determination of the overall thresholds for the one-, two-, three-, and four-cycle conditions. The experiment was performed for the original pattern illustrated in Figure 6 and repeated for the mirror image of this pattern and for the one-, two-, and three-cycle conditions of the mirror image.

Results

Thresholds for the single-cycle condition are plotted independently for the four frequencies (see Figure 7) of modulation in Figure 9. These thresholds represent the combined data for the four observers. In paired t tests, thresholds for the conditions with radial frequencies of 22/8, 22/7, and 22/3 were not statistically different from the condition 22/4, to which they were normalized, for the original, $t(3) = 1.461$, $p = 0.2402$; $t(3) = 2.194$, $p =$

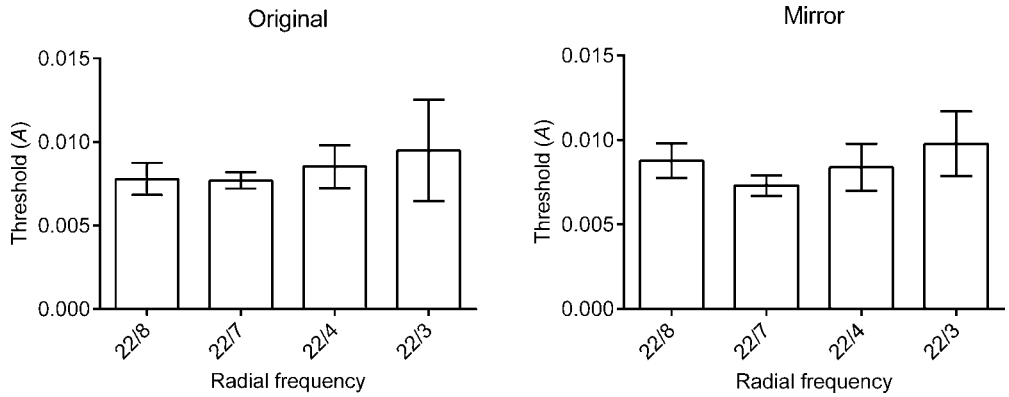

Figure 9. Normalized thresholds for single-cycle conditions. Error bars are 95% confidence intervals. There was no statistically significant difference in threshold across the patterns with different frequencies of modulation if the amplitudes are normalized such that the maximum orientation difference for circular is equated at the same nominal amplitude.

0.1158; $t(3) = 0.8896$, $p = 0.4392$, and mirror image, $t(3) = 0.7966$, $p = 0.4839$; $t(3) = 0.1902$, $p = 0.1534$; t(3) = 2.067, $p = 0.1306$, conditions.

Threshold plotted against the number of cycles of modulation are presented in Figure 10. The data, plotted in log-log coordinates, is seen to conform to a power function for each of the observers for both the original and mirror images of the pattern. The data for the original patterns are plotted as filled red circles and the fit to these data as a solid red line. The thresholds for the mirror image are plotted as open blue squares and the fit as a solid blue line. The predictions for probability summation are plotted as dashed lines. The rate of decrease of the thresholds exceeds the probability summation predictions in all cases. The means of the power function indices across the four observers are −0.72 ±0.16 (95% confidence intervals) and −0.75 (±0.11) for the original and mirror image data, respectively. The means of the indices predicted for probability summation are −0.44 (±0.04) and −0.45 (±0.07) for the same patterns. The indices of the probability summation predictions are the negative

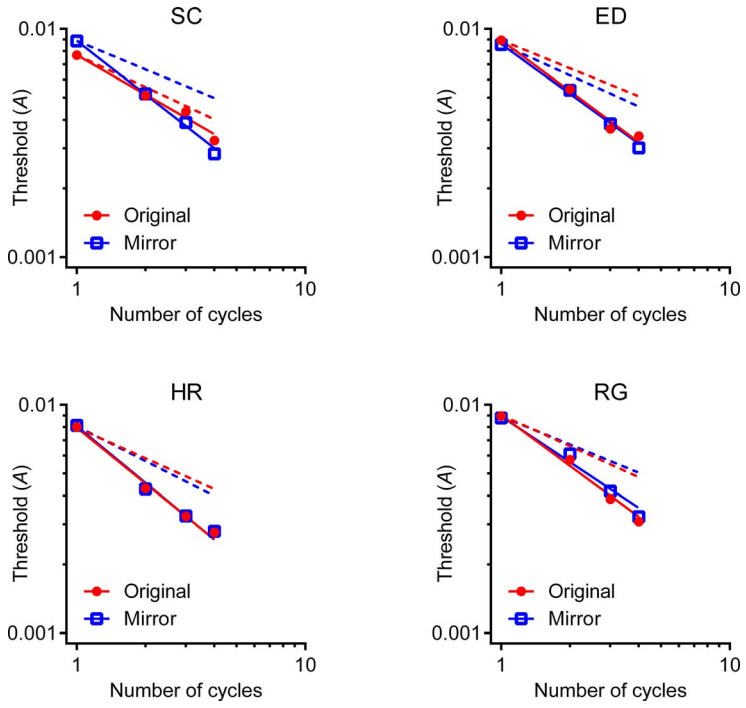

Figure 10. Integration in irregular RF patterns. Thresholds for the detection of modulation in the irregular patterns are plotted against the number of cycles on the pattern. Thresholds for the original pattern are plotted as filled red circles and the mirror images as open blue squares. Fitted power functions (solid red and blue lines, respectively) represent the reduction in threshold with increasing number of cycles of modulation well. Dashed lines show probability summation predictions.

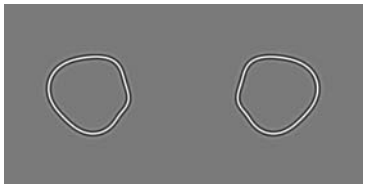

Figure 11. Mirror images of irregular RF patterns. The pattern on the left is created in the manner of the patterns used in Experiment 3, and the pattern on the right is its mirror image. These patterns are handed and cannot be superimposed simply by rotation in the fronto-parallel plane.

reciprocal of the average value of Q across all of the psychometric functions pertaining to the derivation of the power function describing the performance for a particular pattern (i.e., the original or the mirror image). Paired t tests showed that the observed indices were significantly different from the predictions for probability summation for both the original, $t(3) = 4.753$, $p = 0.0177$, and mirror image, $t(3) = 12.25$, $p = 0.0012$, patterns but that the indices for the original and mirror image patterns did not differ significantly, $t(3) = 0.5269$, $p = 0.6348$.

Discussion

The results of Experiment 3 confirm that, near their thresholds for detection, single cycles of sinusoidal modulation are equated in salience when their amplitudes of modulation are scaled by the inverse of their frequencies. Under such circumstances, the maximum angular deviation of the paths from circular are equated. Moreover, when cycles of dissimilar frequency of modulation are concatenated at their zero crossings to form irregular patterns, such patterns display the same integration of modulation information around the path as do patterns with constant frequencies of modulation.

Experiment 4: An irregular RF pattern and its mirror image are not discriminable at their thresholds for detection but an irregular pattern and an RF4 are

Introduction

The results of Experiment 3 demonstrate integration of information across cycles of modulation in irregular patterns. This suggests that such patterns are globally processed. Dickinson et al. (2013) showed that conventional RF3 and RF6 patterns could be discriminated at their thresholds for detection but that patterns with a single cycle of modulation could not. It might be said that this particular result could indicate that the differing number of points of maximum curvature allowed discrimination of the patterns. However, patterns with differing frequency but with two cycles of modulation were perfectly discriminated, but patterns with the same frequency of modulation but different numbers of cycles of modulation were not. On the basis of this result, it was conjectured that the irregular patterns might be discriminated by the set of unique angles subtended by adjacent points of maximum convex curvature on the patterns. A recent paper (Schmidtmann et al., 2012), however, has suggested that the integration of information within RF patterns is implemented by templates requiring specific spatial configurations of curvature features. The irregular patterns developed in Experiment 3 provide an opportunity to test this hypothesis. The irregular patterns shown to be integrated in Experiment 3 can be handed in the sense that a mirror image of an irregular pattern might not be superimposable on the original simply by rotation. This is true of the patterns used in this experiment. The original pattern was created by concatenation cycles of modulation with frequencies of 22/4, 22/8, 22/7, and 22/3 and the mirror image patterns by reflection in a vertical plane. Patterns were created uniquely, however, so reflected patterns were never compared directly. The original and mirror image patterns have the same set of subtended angles, but for the two patterns, the angles number off counterclockwise and clockwise, respectively. The frequencies used in the creation of the stimuli were chosen because they gave a subjective sense that the original and mirror image could not be superimposed by rotation. Conversely, if the integration is performed by spatial templates that require a precise and complete representation of the pattern, as suggested by Schmidtmann et al. (2012), then different templates would be required to represent the original and mirror image versions of the irregular pattern. Given that these patterns have been demonstrated to be globally integrated, we might expect that, if they are processed by precise and discrete spatial templates, they would be perfectly discriminated. Equivalent detection and identification data were collected for the original irregular pattern and an RF pattern with normalized amplitudes of modulation for comparison with the data for the mirror image patterns.

Methods

Stimuli

Stimuli for this experiment were original and mirror image versions of the irregular patterns. Examples are shown in Figure 11.

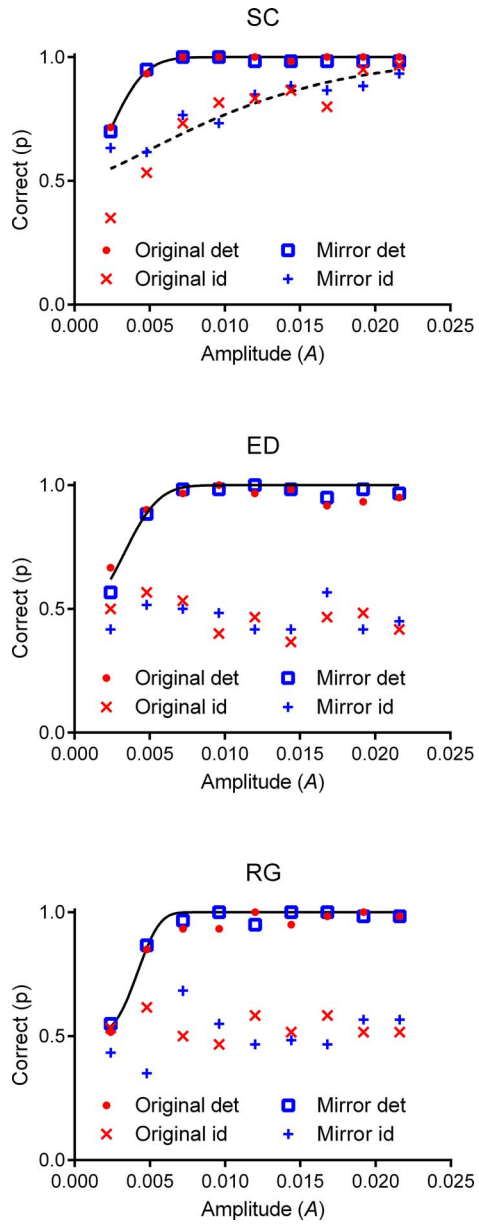

Figure 12. Probabilities for correct detection and identification of modulation in an irregular pattern and its mirror image, plotted against amplitude of modulation. A solid black line represents a Quick function fitted to the combined data for detection of modulation and a dashed black line a fit to the combined data for identification of modulation. Coincidence of the detection data (red dots and open blue squares, fitted with solid black lines) and the identification data (red crosses and blue pluses, fitted with a dashed black line for observer S. C.) would demonstrate an ability to discriminate between the patterns at their thresholds for detection. The observers were not able to discriminate between the mirror image patterns at their thresholds for detection.

Procedure

The experiment used a 2x2IFC task. Trials incorporating each of the two patterns, original and mirror image, were interleaved within a block. Each trial comprised a modulated test pattern and a circular reference pattern presented in a randomized temporal order. For each trial, the observer was required to report first the interval in which the test pattern was presented and second whether the test pattern was an example of the original pattern or the mirror image pattern. The MOCS was used with nine amplitudes of modulation employed in the test patterns. In each block, 20 trials were performed for each of the nine amplitudes used for the original and mirror image patterns in each of three blocks of trials. The data were collated into responses pertaining to the detection of modulation and identification of the two patterns and the probability of correct response calculated for each of the amplitudes of modulation. Where possible, a Quick function was fitted to the psychometric data. To allow a comparison to stimuli that should be discriminated by the set of angles subtended by adjacent points of maximum curvature, a parallel test was performed using an irregular pattern and an RF4 pattern

Results

The results pertaining to the mirror image pair of stimuli are presented in Figure 12. The probability of correct response is plotted with respect to amplitude of modulation. The amplitude of modulation is equal to the parameter A for the cycle of modulation that has the frequency of 22/4. Other cycles of modulation have their amplitudes scaled by the inverse of the ratio of their frequencies to 22/4. A solid black line represents a Quick function fitted to the combined detection data for the mirror image patterns and a dashed black line a fit to the combined identification data. Perfect discrimination of these stimuli (discrimination at their thresholds for detection) would be indicated by coincidence of these two fitted lines and would be consistent with analysis of the patterns in discrete templates. However, it was not possible to achieve a fit of the discrimination data for two of the three observers, and the discrimination data are clearly not coincident with the fit to the detection data. The two mirror image patterns cannot, therefore, be discriminated at their thresholds for detection.

In contrast to the mirror image patterns, the irregular and RF4 patterns were perfectly discriminated. Figure 13 shows the probabilities for correct performance in detection and identification of irregular and RF4 patterns plotted against amplitude of modulation (all amplitudes were scaled to equate maximum orientation difference from circular with a pattern with 22/4 cycles of modulation in 2π radians).

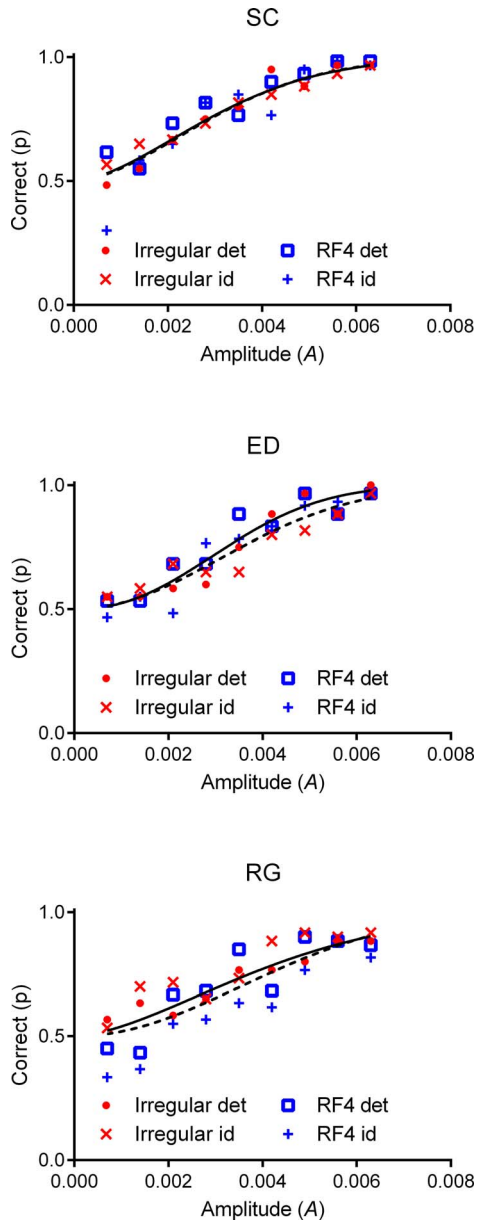

Figure 13. Probabilities for correct detection and identification of modulation in irregular and RF4 patterns, plotted against amplitude of modulation. Data pertaining to the detection and identification of modulation in the irregular (RF4) patterns are plotted in red (blue). Solid lines represent Quick functions fitted to the data for detection of modulation and dashed lines fits to the data for identification of modulation. For all observers, the probabilities for correct identification of the patterns were consistent with being equal to those for detection of modulation across the range of modulation amplitudes used (note the change of range of amplitude compared with those used to test mirror image patterns; Figure 12). The patterns were therefore perfectly discriminated.

The extra sum of squares F tests showed that the functions fitted to the data describing the probability of correct performance in the detection and identification of the irregular and RF4 patterns was consistent with being equal for each observer: SC, $F(2, 104) = 0.01584$, $p = 0.9843$; ED, $F(2, 104) = 1.291$, $p = 0.2794$; RG, $F(2, 104) = 0.7849$, $p = 0.4588$.

Discussion

Experiment 3 demonstrated that shape information in irregular RF patterns is integrated around the pattern. Despite this demonstration of global processing, Experiment 4 showed that discrimination between an irregular pattern that had no rotational symmetry and its mirror image was not possible at their thresholds for detection of modulation, but an irregular pattern and an RF4 pattern were perfectly discriminated. This suggests that, in the first instance, encoding of such patterns is not performed by spatial templates, as discrete templates would be required to encode each of the original and mirror image patterns. These are somewhat esoteric patterns, and so it remains possible that after prolonged exposure to such patterns, discrete templates for these patterns might be developed. This result does not prove that shape is encoded as a set of angles subtended by adjacent corners on the pattern, as suggested by Dickinson et al. (2013), but it is consistent with this solution.

Conclusions

Conventional RF patterns have been used to demonstrate the integration of information around closed paths. Experiment 1 of this study showed that integration also occurs around patterns with a rectified sinusoidal modulation of radius. It is not, therefore, critical to integration that modulation of radius is sinusoidal. This result argues against models of shape analysis that propose decomposition of their boundaries into a RF spectrum. Experiment 1 also demonstrated, across pattern types, that the maximum orientation difference from circular on RF patterns with the same number of cycles of modulation is a constant at threshold. This implies that it is this quantity that defines the salience of the individual cycles of the patterns. Although it is true that orientation histograms (with a uniform sampling interval) would also be the same, Dickinson et al. (2012) previously showed that, at detection threshold, conventional RF patterns with the same number of cycles of modulation but differing frequencies also have the same maximum orientation difference from circular, ruling out the possibility of integration across the orientation histograms defining salience. For the small amplitudes of modulation used in this study, the maximum orientation difference from

circular is proportional to amplitude within a pattern type and therefore is interchangeable with amplitude when considering the index of the power function that is used to test for integration. Across pattern types, however, the maximum orientation difference from circular is equated at threshold only if the full (peak-to-peak) amplitudes are equated. Other properties, such as maximum curvature on the path, were not constant at threshold. On balance, it appears that it is the maximum orientation difference from circular that determines the salience of a single cycle of modulation.

Experiment 2 showed that patterns with sinusoidal, positively rectified, or negatively rectified modulation, with the same rotational symmetry, could not be discriminated at their thresholds for detection. Dickinson et al. (2013) have previously shown that patterns with single cycles of RF3 and RF6 modulation cannot be discriminated at their thresholds for detection but patterns with two cycles of modulation can. Moreover, patterns with differing numbers of cycles of modulation of the same frequency were not perfectly discriminated. Dickinson et al. concluded that the property of the patterns that allowed for perfect discrimination between RF3 and RF6 patterns was the differing angle subtended at the center of the pattern by adjacent points of maximum convex curvature, or corners (at detection threshold, the patterns had no points of curvature concave with respect to the center of the pattern). This leaves us in the somewhat paradoxical situation that the maximum orientation difference from circular determines the salience of the pattern but discrimination of the patterns at threshold relies on a property derived from determination of the positions of points of maximum convex curvature. The results of Experiment 2 support this position, suggesting that encoding of the positions of the points of maximum convex curvature on the path occurs at amplitudes of modulation at which the analysis of the magnitude of the curvature at such points is not possible and, therefore, that the points of maximum curvature are critical to a rudimentary but efficient analysis of shape. Certainly, examination of the patterns in the right-hand column of Figure 2 leaves the subjective impression that the perceived orientation of the pattern is determined by the positions of the points of maximum convex curvature, yet at threshold, the differences in curvature of these points are not apparent. One resolution to this paradox might be that the orientations at the points of maximum deviation from circularity on the path are determined first and then paired by angle detectors, the vertices of which would then indicate the polar positions of the points of maximum curvature. There is some neurophysiological evidence for a preponderance of angle detectors in cortical area V4, an area implicated in object processing (Carlson, Rasquinha, Zhang, & Connor, 2011).

Prior to this study, experimentation using RF patterns to demonstrate integration of shape information has always used patterns with a constant frequency of modulation. Experiment 3 of this study, however, demonstrated that information is similarly integrated around patterns that incorporate cycles of sinusoidal information of differing frequency and, given that Dickinson et al. (2013) demonstrated that patterns with at least two cycles of modulation can be discriminated at their threshold for detection, it might be assumed that more complex patterns might be discriminated on the basis of the angles subtended at the center of the pattern by adjacent points of maximum convex curvature. If patterns are discriminated by the content of the set of angles subtended by adjacent points of maximum curvature, then a pattern should not be perfectly discriminated from its mirror image because the sets are identical. The results of Experiment 4 support this argument, showing that an irregular RF pattern cannot be discriminated from its mirror image at its threshold for detection but can be discriminated from an RF4 pattern.

It must be recognized, however, that the results of this study pertain specifically to the analysis of patterns at or near their thresholds for detection. The utility of such studies is rooted in the premise that cues to shape other than those under investigation are reduced in salience to such an extent that they do not affect the measurements made, allowing specific mechanisms of analysis to be targeted. Models of analysis of shape well above the threshold for detection differ from those proposed here. As previously mentioned, Pasupathy and Connor (2002) encode shape via a trajectory in curvature versus polar angle space. We find that, near threshold, absolute curvature is not encoded, effectively collapsing the curvature axis. Further, however, we find an indifference of the mechanism to the order in which the polar angles between curvature features occur, counterclockwise or clockwise. For suprathreshold shapes, analysis of curvature around RF patterns may indeed be important to object recognition. Recent psychophysical adaptation studies have suggested that points of maximum and minimum curvature and curvature inflections are all important to the analysis of shape (Bell, Hancock, Kingdom, & Peirce, 2010; Bell, Sampasivam, McGovern, Meso, & Kingdom, 2014). Bell et al. (2010) segregated parts of high-amplitude RF patterns that represented regions of convex and concave curvature on the path and also parts that included a point at which the curvature changed sign, a point of inflection. Aftereffects of adaptation to these sampled patterns were demonstrated in patterns that had different amplitudes of modulation. It was

shown that if the adaptors were alternated during the adapting periods (for example, alternation between the convex and concave parts of the pattern every 500 ms in each 2-s adapting period), the effects of adaptation were cumulative, and this was interpreted as evidence for the global processing of RF patterns at suprathreshold amplitudes of modulation. Similarly, it was shown that alternating between the parts of the pattern with opposite polarity points of inflection also produced cumulated aftereffects. Bell et al. (2014) further investigated the points of inflection, demonstrating that paths that included points of inflection induced aftereffects that were larger in magnitude for same-contrast polarity adaptor test pairs than for opposite-contrast polarities. The tilt aftereffect magnitude was shown to be robust to change in contrast polarity, allowing the adaptation to the points of inflection to be interpreted as distinct from the tilt aftereffect. A comparable argument allowed Bell, Gheorghiu, Hess, and Kingdom (2011) to infer the existence of a stage of integration of shape information that is polarity selective. These adaptation methods are not without their limitations, however, in particular the confounding effects of local orientation adaptation (Blakemore & Over, 1974; Dickinson, Almeida, et al., 2010; Dickinson & Badcock, 2013; Dickinson, Harman et al., 2012; Dickinson, Mighall et al., 2012) that might account for some of the adaptation effects observed in RF patterns, but they do suggest the availability of a broader range of cues at suprathreshold levels. The current study introduces features to the patterns under investigation that do not exist on RF patterns. Curvature discontinuities are introduced to the path, and it is shown that these features do not compromise integration of information. Further, it is shown that irregular RF patterns are also processed globally providing for a continuum of shapes that might be exploited as stimuli in adaptation experiments and other experimental paradigms.

Keywords: radial frequency patterns, shape, form, threshold, detection, discrimination, global integration

Acknowledgments

This research was supported by Australian Research Council Grants DP1097003, DP110104553, and DP130102580 to D. R. B.

Commercial relationships: none.
Corresponding author: J. Edwin Dickinson.
E-mail: edwin.dickinson@uwa.edu.au.
Address: School of Psychology, University of Western Australia, Crawley, Perth, WA, Australia.

Footnote

[1] This test compares two models, the first being that of a global fit and the second that the two curves are distinct. It assumes a null hypothesis that the global fit is the best and uses statistical hypothesis testing, using a criterion of $p < 0.05$, to examine if there is sufficient evidence to reject this hypothesis, The degrees of freedom in the numerator in the calculation of the F ratio is 2, the difference in the number of degrees of freedom in the null hypothesis model and the alternative model. The degrees of freedom in the denominator is the number of degrees of freedom in alternative hypothesis (Motulsky & Christopoulos, 2004). For the F tests, the probabilities of correct detection across blocks of trials were treated as independent, and therefore, each fitted function has 54 samples of probability of correct response (six blocks of nine points on the psychometric function). There were two free parameters in the fit and therefore 52 degrees of freedom or 104 for the two curves. The global fit has two fewer degrees of freedom.

References

Almeida, R. A., Dickinson, J. E., Maybery, M. T., Badcock, J. C., & Badcock, D. R. (2010a). A new step towards understanding Embedded Figures Test performance in the autism spectrum: The radial frequency search task. *Neuropsychologia, 48*, 374–381.

Almeida, R. A., Dickinson, J. E., Maybery, M. T., Badcock, J. C., & Badcock, D. R. (2010b). Visual search performance in the autism spectrum II: The radial frequency search task with additional segmentation cues. *Neuropsychologia, 48*, 4117–4124.

Almeida, R. A., Dickinson, J. E., Maybery, M. T., Badcock, J. C., & Badcock, D. R. (2013). Visual search targeting either local or global perceptual processes differs as a function of autistic-like traits in the typically developing population. *Journal of Autism and Developmental Disorders, 43*, 1272–1286.

Almeida, R. A., Dickinson, J. E., Maybery, M. T., Badcock, J. C., & Badcock, D. R. (2014). Enhanced global integration of closed contours in individuals with high levels of autistic-like traits. *Vision Research, 103,* 109–115.

Attneave, F. (1954). Some informational aspects of visual perception. *Psychological Review, 61*, 183–193.

Badcock, D. R. (1988). Discrimination of spatial phase changes: Contrast and position codes. *Spatial Vision, 3*, 305–322.

Badcock, D. R., & Derrington, A. M. (1989). Detecting the displacements of spatial beats: No role for distortion products. *Vision Research, 29*, 731–739.

Bell, J., & Badcock, D. R. (2008). Luminance and contrast cues are integrated in global shape detection with contours. *Vision Research, 48*, 2336–2344.

Bell, J., Badcock, D. R., Wilson, H. R., & Wilkinson, F. (2007). Detection of shape in radial frequency contours: Independence of local and global form information. *Vision Research, 47*, 1518–1522.

Bell, J., Dickinson, J. E., & Badcock, D. R. (2008). Radial frequency adaptation suggests polar-based coding of local shape cues. *Vision Research, 48*, 2293–2301.

Bell, J., Gheorghiu, E., Hess, R. F., & Kingdom, F. A. A. (2011). Global shape processing involves a hierarchy of integration stages. *Vision Research, 51*, 1760–1766.

Bell, J., Hancock, S., Kingdom, F. A. A., & Peirce, J. W. (2010). Global shape processing: Which parts form the whole? *Journal of Vision, 10*(6):16, 1–13, http://www.journalofvision.org/content/10/6/16, doi:10.1167/10.6.16. [PubMed] [Article]

Bell, J., Sampasivam, S., McGovern, D. P., Meso, A. I., & Kingdom, F. A. A. (2014). Contour inflections are adaptable features. *Journal of Vision, 14*(7):2, 1–14, http://www.journalofvision.org/content/14/7/2, doi:10.1167/14.7.2. [PubMed] [Article]

Biederman, I., & Cooper, E. E. (1991). Priming contour-deleted images: Evidence for intermediate representations in visual object recognition. *Cognitive Psychology, 23*, 393–419.

Blakemore, C., & Over, R. (1974). Curvature detectors in human vision? *Perception, 3*, 3–7.

Carlson, E. T., Rasquinha, R. J., Zhang, K., & Connor, C. E. (2011). A sparse object coding scheme in area V4. *Current Biology: CB, 21*, 288–293.

Connor, C. E. (2004). Shape dimensions and object primitives. In L. M. Chalupa & J. S. Werner (Eds.), *The visual neurosciences* (Vol. 2., pp. 1080–1089). Cambridge, MA: MIT press.

Dickinson, J. E., Almeida, R. A., Bell, J., & Badcock, D. R. (2010). Global shape aftereffects have a local substrate: A tilt aftereffect field. *Journal of Vision, 10*(13):5, 1–12, http://www.journalofvision.org/content/10/13/5, doi:10.1167/10.13.5. [PubMed] [Article]

Dickinson, J. E., & Badcock, D. R. (2013).. *Frontiers in Psychology, 4*, 472.

Dickinson, J. E., Bell, J., & Badcock, D. R. (2013). Near their thresholds for detection, shapes are discriminated by the angular separation of their corners. *PLoS One, 8*, e66015.

Dickinson, J. E., Han, L., Bell, J., & Badcock, D. R. (2010). Local motion effects on form in radial frequency patterns. *Journal of Vision, 10*(3):20, 1–15, http://www.journalofvision.org/content/10/3/20, doi:10.1167/10.3.20. [PubMed] [Article]

Dickinson, J. E., Harman, C., Tan, O., Almeida, R. A., & Badcock, D. R. (2012). Local contextual interactions can result in global shape misperception. *Journal of Vision, 12*(11):3, 1–20, http://www.journalofvision.org/content/12/11/3, doi:10.1167/12.11.3. [PubMed] [Article]

Dickinson, J. E., McGinty, J., Webster, K. E., & Badcock, D. R. (2012). Further evidence that local cues to shape in RF patterns are integrated globally. *Journal of Vision, 12*(12):16, 1–17, http://www.journalofvision.org/content/12/12/16, doi:10.1167/12.12.16. [PubMed] [Article]

Dickinson, J. E., Mighall, H. K., Almeida, R. A., Bell, J., & Badcock, D. R. (2012). Rapidly acquired shape and face aftereffects are retinotopic and local in origin. *Vision Research, 65,* 1–11.

Feldman, J., & Singh, M. (2005). Information along contours and object boundaries. *Psychological Review, 112*(1), 243–252.

Field, D. J., & Hayes, A. (2004). Contour integration and the lateral connections of V1 neurons. In L. M. Chalupa & J. S. Werner (Eds.), *The visual neurosciences* (Vol. 2., pp. 1069–1079). Cambridge, MA: MIT Press.

Field, D. J., Hayes, A., & Hess, R. F. (1993). Contour integration by the human visual system: Evidence for a local "association field." *Vision Research, 33*, 173–193.

Hoffman, D. D., & Richards, W. A. (1984). Parts of recognition. *Cognition, 18,* 65–96.

Hubel, D. H., & Wiesel, T. N. (1959). Receptive fields of single neurones in the cat's striate cortex. *Journal of Physiology, 148,* 574–591.

Hubel, D. H., & Wiesel, T. N. (1968). Receptive fields and functional architecture of monkey striate cortex. *Journal of Physiology, 195*, 215–243.

Julesz, B. (1962). Visual pattern discrimination. *IRE Transactions on Information Theory, 8*, 84–92.

Kovacs, I., & Julesz, B. (1993). A closed curve is much more than an incomplete one: Effect of closure in figure-ground segmentation. *Proceedings of the National Academy of Sciences, USA, 90*, 7495–7497.

Lennie, P. (1998). Single units and visual cortical organization. *Perception, 27*, 889–935.

Li, W., & Gilbert, C. D. (2002). Global contour saliency and local colinear interactions. *Journal of Neurophysiology, 88*, 2846–2856.

Loffler, G. (2008). Perception of contours and shapes: Low and intermediate stage mechanisms. *Vision Research, 48*, 2106–2127.

Loffler, G., Wilson, H. R., & Wilkinson, F. (2003). Local and global contributions to shape discrimination. *Vision Research, 43*, 519–530.

Motulsky, H., & Christopoulos, A. (2004). *Fitting models to biological data using linear and nonlinear regression: A practical guide to curve fitting*. Oxford, UK: Oxford University Press.

Mullen, K. T., Beaudot, W. H. A., & Ivanov, I. V. (2011). Evidence that global processing does not limit thresholds for RF shape discrimination. *Journal of Vision, 11*(3):6, 1–21, http://www.journalofvision.org/content/11/3/6, doi:10.1167/11.3.6. [PubMed] [Article]

Pasupathy, A., & Connor, C. E. (1999). Responses to contour features in macaque area V4. *Journal of Neurophysiology, 82*, 2490–2502.

Pasupathy, A., & Connor, C. E. (2001). Shape representation in area V4: Position-specific tuning for boundary conformation. *Journal of Neurophysiology, 86*, 2505–2519.

Pasupathy, A., & Connor, C. E. (2002). Population coding of shape in area V4. *Nature Neuroscience, 5*, 1332–1338.

Poirier, F. J. A. M., & Wilson, H. R. (2006). A biologically plausible model of human radial frequency perception. *Vision Research, 46*, 2443–2455.

Quick, R. F., Jr. (1974). A vector-magnitude model of contrast detection. *Kybernetik, 16*, 65–67.

Schmidtmann, G., Kennedy, G. J., Orbach, H. S., & Loffler, G. (2012). Non-linear global pooling in the discrimination of circular and non-circular shapes. *Vision Research, 62*, 44–56.

Tan, K. W. S., Dickinson, J. E., & Badcock, D. R. (2013). Detecting shape change: Characterizing the interaction between texture-defined and contour-defined borders. *Journal of Vision, 13*(14):12, 1–16, http://www.journalofvision.org/content/13/14/12, doi:10.1167/13.14.12. [PubMed] [Article]

Watson, A. B., & Robson, J. G. (1981). Discrimination at threshold: labelled detectors in human vision. *Vision Research, 21*, 1115–1122.

Wilkinson, F., Wilson, H. R., & Habak, C. (1998). Detection and recognition of radial frequency patterns. *Vision Research, 38*, 3555–3568.

Wilson, H. R. (1980). A transducer function for threshold and suprathreshold human vision. *Biological Cybernetics, 38*, 171–178.

Wilson, H. R. (1985). Discrimination of contour curvature: Data and theory. *Journal of the Optical Society of America A, 2*, 1191–1199.

Wilson, H. R., & Richards, W. A. (1989). Mechanisms of contour curvature discrimination. *Journal of the Optical Society of America A, 6*, 106–115.

Appendix

Observer	RF/+ve	RF/−ve	+ve/−ve
SC	$F(2, 104) = 134.3$, $p < 0.0001$	$F(2, 104) = 61.08$, $p < 0.0001$	$F(2, 104) = 24.86$, $p < 0.0001$
ED	$F(2, 104) = 81.50$, $p < 0.0001$	$F(2, 104) = 105.1$, $p < 0.0001$	$F(2, 104) = 27.11$, $p < 0.0001$
HR	$F(2, 104) = 94.95$, $p < 0.0001$	$F(2, 104) = 88.82$, $p < 0.0001$	$F(2, 104) = 81.04$, $p < 0.0001$
TM	$F(2, 104) = 72.37$, $p < 0.0001$	$F(2, 104) = 35.34$, $p < 0.0001$	$F(2, 104) = 18.90$, $p < 0.0001$

Table A1. Results of extra sum of squares F tests of performance in detection versus discrimination of patterns. *Notes:* Psychometric data describing performance in the detection and discrimination of the pairs of patterns types (RF/+ve, RF/−ve, and +ve/−ve) were fitted with Quick functions. The extra sum of squares F tests showed that the fits to the data describing the probabilities for correct response for detection and discrimination of modulation were statistically different functions.